Tellus (2006), 58A, 445–455
Printed in Singapore. All rights reserved

TELLUS

Validation of mesoscale low-level winds obtained by dynamical downscaling of ERA40 over complex terrain

By N. ŽAGAR[1]*, M. ŽAGAR[2], J. CEDILNIK[2], G. GREGORIČ[2] and J. RAKOVEC[1], [1]*University of Ljubljana, Ljubljana, Slovenia;* [2]*Environmental Agency of Slovenia, Ljubljana, Slovenia*

(Manuscript received 2 June 2005; in final form 9 February 2006)

ABSTRACT

The mesoscale numerical weather prediction model ALADIN has been applied for downscaling ERA40 data onto a 10 km grid covering the complex terrain of Slovenia. The modelled wind field is compared with the time-series of observations at 11 stations. In addition to traditional scores (root-mean-square error, mean absolute error, anomaly correlation), a frequency-domain comparison is carried out in order to explore aspects of the mesoscale model performance other than that depicted by the conventional statistics. The verification period is the Special Observing Period of the Mesoscale Alpine Program (MAP-SOP), for which ECMWF reanalyses including MAP-SOP observations are available every 3 hr on a ∼40 km grid.

Traditional scores indicate that the downscaling has been successful. Scores are little dependent on the nesting strategy (direct versus two-step nesting), in spite of a ratio of horizontal resolutions between ERA40 and ALADIN as large as 12. The model performs best at mountaintop stations, characterized by over 80% of their spectral power in motions with longer than diurnal periods. A majority of stations is, however, located in the complex terrain where around 40% of the spectral wind power is contained in the subdiurnal frequency range. This part of the spectrum is significantly underestimated by the model, indicating that the downscaling is predominantly a dynamical adjustment to the new terrain. At the same time, the MAP-SOP reanalyses of the ECMWF model include relatively more power in the subdiurnal frequency range than ALADIN. However, these subdiurnal oscillations do not agree with observations and their removal improves conventional scores for the MAP-SOP wind data.

It is suggested that a frequency-domain comparison is a useful complement to the conventional statistics and it enables a more physical insight into a mesoscale model performance.

1. Introduction

Mesoscale models are commonly used to deduce the wind field in complex terrain by dynamically downscaling reanalysis data, global numerical weather prediction (NWP) or climate models. A typical jump in the horizontal resolution is from about one to two degrees down to about ten to few tens of kilometres. Downscaling introduces new scales, both spatial and temporal; that is, enhanced variability arises due to a common action of model dynamics and physics at a higher resolution. Predictable mesoscale phenomena are intimately linked to the large scale forcing (e.g. foehn, bora, frontal convection, blocking and channelling), terrain forcings (e.g. valley and slope winds) and surface heterogeneities (e.g. sea-breeze circulations). In complex terrains, spatial variability is introduced first. Temporal variability is enhanced through thermal circulations (i.e. valley and slope winds and sea breezes).

Verification of these mesoscale flows is an important issue for which adequate approaches still need to be defined. Traditional verification scores, such as mean-absolute error (MAE) and root-mean-square error (RMSE) appear to be insufficient, as small timing errors due to fast propagating mesoscale features easily contaminate the score thus making it incapable of showing a positive impact of the increasing horizontal resolution (e.g. Mass et al., 2002). Conventional measures can hardly illuminate particular modelling aspects contributing to the (un)reality of simulated circulations; physical understanding has to be searched through additional parameters and particular cases. Case studies, in particular, effectively illustrate a positive impact of increasing horizontal resolution (e.g. Žagar and Rakovec, 1999).

The main purpose of this study is to quantify the mesoscale wind variability introduced by the dynamical downscaling of ERA40 (reanalyses of the European Centre for Medium-Range Weather Forecast, ECMWF) by a mesoscale NWP model

*Corresponding author.
e-mail: nedjeljka.zagar@fmf.uni-lj.si
DOI: 10.1111/j.1600-0870.2006.00186.x

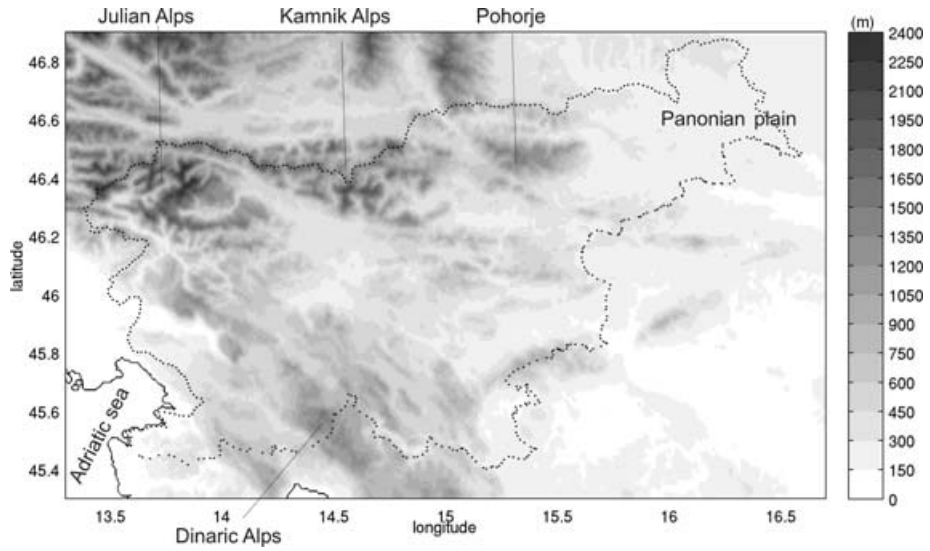

Fig. 1. Orography of Slovenia at 1 km resolution.

(ALADIN; Bubnova et al., 1995) and to verify it against observed variability in a complex terrain.

We aim at understanding what mesoscale processes are resolved by the downscaling. For this purpose we combine conventional verification scores such as MAE, RMSE and anomaly correlation (AC) with a frequency-domain-based comparison. Spectral decomposition in the temporal domain allows quantifying circulation in terms of subdiurnal, diurnal and longer than diurnal (LTD) periods. The distribution of spectral power in three frequency bands provides information about the exposure of measurement locations to non-local features and thus the model ability to reconstruct the observations.

The area of our interest is the complex terrain of Slovenia, at the junction of the eastern Alps, the Dinaric Alps and the Adriatic sea (Fig. 1). A majority of verifying stations is located in valleys and basins; thus we expect to find a significant part of energy at the mesoscale, corresponding to the diurnal and subdiurnal timescales. We aim at quantifying this less predictable part of the wind spectrum and the ability of the ALADIN model to reconstruct the observed spectra.

Combined verification measures are furthermore used to investigate the nesting strategy. The model setup is defined to ensure that the domain size is such that the atmosphere, as resolved by ALADIN, is not distorted or damped by the lateral boundary conditions (LBC); that is, the domain must be large enough to allow for the development of mesoscale features, which can be simulated by the model. The domain, on the other hand, must not be larger than that. Optimal nesting strategy is thus an important issue of seeking an optimal compromise between the dynamical accuracy and computational cost of the dynamical downscaling, especially for regional simulations of climate scenarios.

For verification period we select the interval in autumn 1999: the Mesoscale Alpine Program−Special Observing Period (MAP-SOP; Bougeault et al., 2001). The latest ECMWF data assimilation system was employed on MAP-SOP measurements to produce a special reanalysis data set (Keil and Cardinali, 2004). Although not many additional measurements were available in Slovenia and surface wind observations were not assimilated, MAP-SOP reanalyses, available every 3 hr on a ∼40 km grid, provide information about the quality of the state-of-the-art analysis system, as compared to the mesoscale model used as a 'magnifying glass' for ERA40 data at a three times lower horizontal resolution.

The paper is organized as follows. Details of methodology are presented in Section 2. Here we describe observing stations, nesting strategies and verification methods. Results are discussed in Section 3. First we present conventional verification scores and discuss their sensitivity with respect to the mesoscale domain definition. Then we compare observed spectra with those obtained by the ALADIN model and from the MAP-SOP reanalysis data. In particular, we discuss the subdiurnal variability according to the two models. The main results and their implications are summarized in Section 4.

2. Methodology

2.1. Model and nesting strategy

Driving ERA40 fields (Kållberg et al., 2004) have a higher vertical but a much lower horizontal resolution than the ALADIN model. ALADIN is usually run at around 10 km resolution, while ERA40 has a grid spacing of about 120 km). In the vertical direction there are 60 model levels in ERA40 while about a half

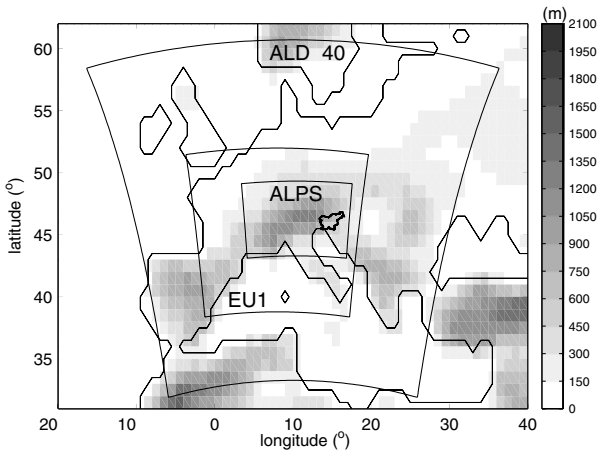

Fig. 2. Domains of the ALADIN model used for simulations experiments. The orography and land–sea mask are from ERA40.

of that number (31) is used in our ALADIN application. The main difference is in the upper troposphere and the stratosphere (i.e. 29 levels in ERA40 above 200 hPa compared to 9 levels in ALADIN), which does not have great importance to our study of the surface wind climatology. Details and numerous references about the ALADIN model, which is used operationally at several European national weather services, are available at http://www.cnrm.meteo.fr/aladin.

Initial and LBC from ERA40 are available with a 6 hr frequency. The pre-processing step includes vertical and horizontal interpolation, which is followed by a digital filter initialization, a sequence of steps similar to that used in operational applications where ALADIN is coupled to the global ARPEGE model. The output is saved every 3 hr. Wind at 10 m level, used for the comparison with observations, is obtained by vertical interpolation between the lowest model level and the surface, making use of similarity theory. This is a standard way of obtaining the wind field at the surface in NWP applications, and in the present study we do not aim at addressing the issue of the applicability of similarity theory (e.g. assumptions about a steady state, plane terrain, uniform roughness, etc.).

We compare two nesting strategies and three horizontal domains, shown in Fig. 2. Two domains are directly nested to ERA40 and they have a horizontal resolution of 10 km. Their only difference is the positioning of the lateral boundaries. The larger domain (denoted EU1) consists of 188×188 physically relevant points covering large part of Europe and the western Mediterranean. The smaller domain is denoted ALPS and it includes 104×68 modelling points. Neither of these two domains is centred over Slovenia but shifted to the west relative to this region. The reason is that the wind climatology of the area of interest is mainly due to the westerly flow impinging on the Alps. Interaction of the flow with the Alps, flow deflection, blocking and lee-side developments determine the mesoscale wind characteristics (e.g. Brzović, 1999).

Table 1. List of various experiments mentioned in the text

Experiment name	Initial/Lateral boundaries	Resolution
ALD-40	ERA40	40 km
ALPS2	ALD-40	10 km
ALPS1	ERA40	10 km
EU1	ERA40	10 km

The ratio of horizontal resolution in ALADIN and ERA40 is 12, a factor that Denis et al. (2003) found to represent an upper limit for a resolution jump between their global and regional models for North America. Therefore, we compare results of the directly nested ALPS domain (hereafter ALPS1) with a simulation where the same domain was imbedded in an intermediate domain comprising Europe and Mediterranean with a horizontal resolution of 40 km (denoted ALD-40). The latter ALPS simulation is denoted ALPS2. The only model change between ALD-40 and ALPS simulations, besides the domain size and horizontal resolution, are the integration time step and timescale of the numerical diffusion, tuned according to well-established relationships.

Various experiments are summarized in Table 1. We shall concentrate on the ALPS domain and mention EU1 results whenever there is a significant difference between the two directly nested simulations (i.e. EU1 and ALPS1). Our results can be compared with a recent study by Beck et al. (2004), where it was reported that precipitation simulations by the ALADIN model over the Alps are comparably successful with direct nesting (with resolution jump for factor 10) and double nesting strategy.

Initial conditions interpolated from ERA40 hardly contain any significant information on scales below one degree (or even lower) horizontal resolution. But after the forecast has started the mesoscale part of the kinetic energy spectrum quickly develops. Energy builds up mainly between forecast hours three to six and changes after 10 hr of forecast are negligible. Thus we take a 12 hr period for the model spin-up time. Spectra of the kinetic energy indicate that below 150 km kinetic energy is equally divided between divergent and rotational parts. The slope of the spectrum (averaged throughout the free troposphere) has a wavenumber dependence in the mesoscale range closer to k^{-3} than to the expected $k^{-5/3}$ law (not shown). However, close to the surface spectra flatten, illustrating the strength of the surface forcing. Here, much less energy, as compared to the tropospheric average, is found at scales above ∼180 km, and there is relatively more energy below this scale. Figure 3 illustrates this shift for the vorticity and divergence fields.

Downscaling is carried out by reinitializing the model every 2 d (days). An option with daily reinitialization has been tested but it did not bring about improvements. Another option is a continuous run, but results of this experiment produced worse scores

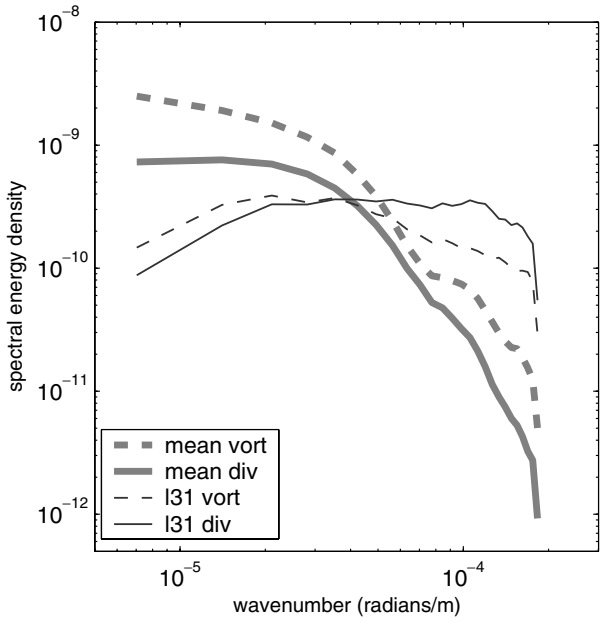

Fig. 3. Spectra for vorticity (dashed line) and divergence (full line) averaged for the 70 d period and within model levels 8–18 (4–9 km) (thick line) and for the lowest model level (level 31, at ∼20 m) (thin line).

than those from a reinitialized simulation, in agreement with other studies indicating that periodic reinitialization of regional models provides better downscaling results than the continuous simulation (e.g. Qian et al., 2003).

2.2. *Wind observations and verification strategy*

The verification period covers 70 d of the MAP-SOP, 7 September to 15 November 1999. Since ECMWF reanalyses for the MAP-SOP period (hereafter MAP reanalyses) are provided with the same time frequency which we used for ALADIN outputs, a comparison of the two data sets illustrates the gain of running the 10 km forecast model in comparison to the analysis system at four times lower resolution. In addition, we verify the ALADIN forecasts at 40 km (ALD-40) against MAP reanalysis to compare dynamical downscaling against data assimilation at the same horizontal resolution.

Like ERA40, MAP reanalyses are available at 60 model levels, and the lowest level is about 10 m above the surface. The post-processing to 10 m height in the ECMWF model is dependent on the roughness length of the underlying surface. Vertical interpolation of the wind speed is performed between model level 58, at ∼70 m above the surface, and the surface using similarity profiles, while the wind direction is taken from the lowest model level (level 60). At Slovenian stations this results in the 10 m wind speed between that at model levels 60 and 59.

A large improvement in resolving orography by increasing horizontal resolution from 40 km to 10 km is revealed in Fig. 4. In contrast to the 40 km grid used for MAP reanalyses, a 10 km ALADIN orography contains all major topographic features of Slovenia: high Julian Alps, Kamnik and Pohorje mountains located east of it, the northern part of the Dinaric Alps and basins in between.

Figure 4 also shows 11 stations selected for verification. The criterion for the station selection was the record completeness; selected stations contain no or only a few missing data during the MAP-SOP. This is especially important because of the spectral decomposition. Few missing records were interpolated linearly. Locations of the stations are representative for high elevation plains and mountain summits exposed to upper-air winds (RO, KM, LI), valleys, sheltered basins or plains (SG, NM, BI, PS, BR, LJ, MS) and coastal sites (PO). Throughout the rest of the paper we refer to these three groups as representative of

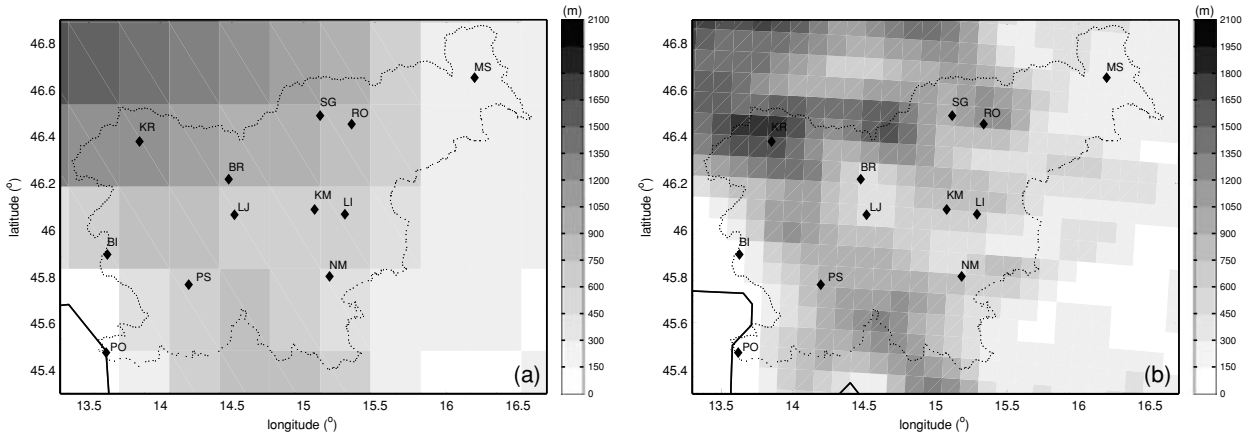

Fig. 4. Orography of Slovenia as represented by (a) the ∼40 km ECMWF model, and (b) the ALADIN model with a 10 km horizontal resolution. Two letter codes designate names of stations used for verification and referenced in the text: SG-Slovenj Gradec, RO-Rogla, MS-Murska Sobota, NM-Novo Mesto, LI-Lisca, KM-Kum, LJ-Ljubljana, BR-Brnik, PS-Postojna, PO-Portorož and BI-Bilje.

exposed mountain locations, coastal circulations and the complex terrain. There are more stations measuring the wind, but those were excluded from the final analysis for the above-mentioned and other reasons. In particular, some mountain stations were eventually excluded because of data holes and poor model scores, a consequence of a very local positioning of the stations.

Mean wind speed during the verification period nowhere exceeds 4 ms^{-1} while it is below 1.5 ms^{-1} at the stations located in basins and valleys. Wind roses are dominated by NE and SW directions, to varying extent modified by local forcings. NE wind direction is related to the northwesterly flow coming over/around the Alps and turning towards the Adriatic (the bora flow), while SW wind directions are frequently a consequence of non-local circulations connected to the cyclones travelling across the northern Europe (e.g. Brzović, 1999; Heimann, 2001). Wind time-series are based on half-hour averages obtained from three 10 min averages. As such, they do not contain random turbulence.

The verification approach is to avoid interpolation of the model outputs but to select, among the four neighbouring model grid points, a point which best corresponds to the position of a measurement site with respect to the surrounding orography. Every change of the computational domain in the spectral ALADIN model affects the orography; this means that verifying points in the model as well as the terrain surrounding locations of measurements are never exactly the same. Due to the spectral orography fit, differences in the relief height between ALPS and EU1 over the area of Slovenia are up to 200 m, but mainly in the range ± 50 m. We have tried to carefully select verification points in various domains to best represent positions of stations with respect to the surrounding orography.

We do not account for the representativeness error due to a difference between a measuring point and a 10×10 km^2 model grid-box average. In many cases wind measurements are exposed to very local influences restricting their spatial representativeness to a radius of only a few hundred metres. Some estimations adduce value of 1 ms^{-1} as representativeness error of the near surface wind speed in a well-mixed boundary layer compared to model simulations in a complex terrain (e.g. Rife et al., 2004). This estimate agrees with results obtained by calculations of deviations of measured wind speeds from high-resolution objective analyses over the Alps (Steinacker et al., 2000).

Conventional verification statistics include bias, AC index, RMSE and MAE. Less conventional information becomes available when time-series are spectrally decomposed to reveal how much of the total energy is related to the circulation on subdiurnal scales, on diurnal and LTD periods. For this purpose we apply the spectral analysis program developed by Ghil et al. (2002). Since we reinitialize the model, ALADIN time-series are not continuous. However, by analysing a continuous run on the same ALADIN domains, we ascertained that reinitialization does not introduce non-meteorological signal that is damaging for the spectra. Time-series contain 560 data and were detrended prior to spectral decomposition. A Bartlett window of width 56 was used for the spectral estimates (see Ghil et al., 2002, for details).

Rife et al. (2004) (henceforth RDL2004) applied a discrete Fourier transformation on the time-series of the observed wind in the complex terrain surrounding Salt Lake City (Utah, USA). They found a relatively small amount of diurnal power at all stations and a significant percentage of power in the subdiurnal band in the valley. Here we make similar estimates for Slovenian stations but we also study the model ability to reconstruct the observed power spectra. In addition, a comparison of spectra at various domains should show whether a close neighbourhood of LBCs distorts mesoscale phenomena developed in the small ALADIN domain (ALPS), as compared to the larger one (EU1). For a comparison with RDL2004, the diurnal range is defined as periods between 22 and 26 hr, the subdiurnal motions comprise periods between 6 and 22 hr and LTD motions are those with periods longer than 26 hr. As discussed in RDL2004, the energy in the subdiurnal range is generated during the model forecast through various landscape forcings and non-linear interactions. Although a detailed investigation of the ALADIN model capability to produce subdiurnal motions is out of the scope of the present paper, it is interesting to see how a large part of the model energy is contained in this frequency range (for whatever reason).

3. Results

3.1. Conventional verification statistics

Figure 5 shows conventional scores, MAE, RMSE and AC, for the meridional wind component for three ALADIN simulations and MAP reanalyses (denoted as ECMWF in figure). A score based on 24 hr persistence forecast (denoted PERS) is added for reference. First of all, comparing ALADIN results with the diurnal persistence-based score and MAP-SOP reanalyses, it is concluded that the downscaling to 10 km has been successful. In particular, stations well exposed to synoptic forcing and with the mean wind speed over 3 ms^{-1} (i.e. RO, LI and KM) are characterized by a large AC and a very poor persistence score. For complex-terrain stations the RMSE of persistence-based forecast is in several cases between the ALADIN and MAP reanalysis results, corroborating the importance of horizontal resolution in complex terrain. Results are very similar for the zonal wind component.

The conventional scores for MAP reanalysis are almost everywhere worse than those for a 10 km ALADIN, in agreement with expectations. A more interesting result is that the ECMWF reanalysis for MAP-SOP period are also less successful than the ALADIN forecasts at the same horizontal resolution. We address this issue separately later in this section.

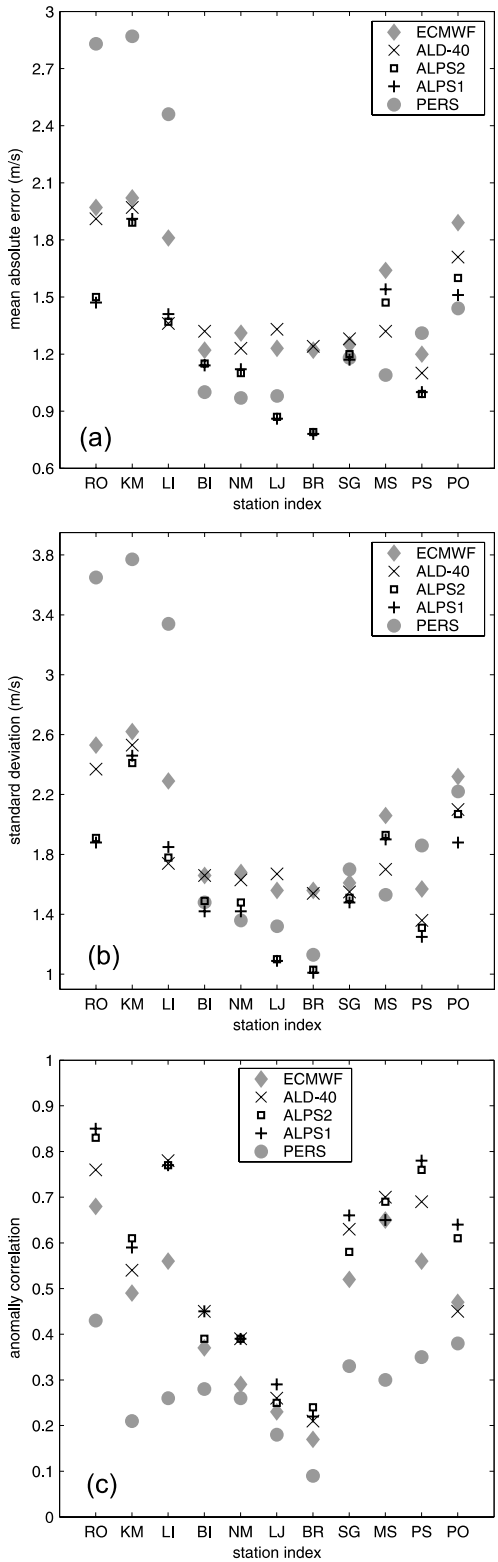

Fig. 5. (a) Mean absolute error, (b) root mean square error and (c) anomaly correlation scores for the meridional wind component at the 11 stations during the MAP-SOP period. Symbols correspond to various experiments, as explained in the text.

Differences between directly (ALPS1) and two-step (ALPS2) nested simulations are not significant at majority of stations, in spite of the jump in horizontal resolution as large as factor 12, in agreement with the results of Beck et al. (2004). A larger difference is obtained for two directly nested simulations (EU1 and ALPS1, not shown), indicating unpredictability of local responses to small variations in lateral boundaries forcing. However, these differences are small at stations located well above local influences (RO, KM and LI). Comparing the time-series from EU1 and ALPS1 simulations, it is found that main differences are associated with significant weather; in these cases both amplitudes and timings of the significant changes of the wind speed and direction are better simulated by the ALPS1 experiment. Errors in strong-wind situations are largest; thus, the impact of the domain size is best represented by the RMSE score (not shown).

Overall the ALPS1 simulation has the best scores, indicating the positive effect of the LB forcing. However, this result may also reflect some model errors and, in particular, insufficiencies of the model physics at a horizontal resolution of 10 km to represent mesoscale processes acting over the complex terrain. It is worth noting that other studies dealing with the domain-size problem for regional model simulations over Europe reached the same conclusion: a smaller domain performed better (e.g. Jones et al., 1995).

Since measurements of the wind direction are often unreliable at low wind speeds, we have separately looked at strong-wind cases defined by wind speeds greater than 3 ms^{-1}. At the mountain stations, strong winds blew 50–60% of the MAP-SOP period, and only 6% of that time at station BR. For strong-wind situations AC is improved with respect to all cases, but the MAE and RMSE scores are made worse at all stations, in average for 10–20%. We also mention that the Alpine valleys are characterized by many days of no wind at all. For example, the wind speed at BR was below 1 ms^{-1} during 58% of the time studied. The ALPS2 simulation is closest to this percentage with 55% of time characterized by wind speed below 1 ms^{-1}, followed by ALPS1 (53%), EU1 (45%), ALD-40 (19%) and MAP reanalysis (11%).

3.2. Spectra in the temporal domain

In Figs. 6–7 we present spectral power distribution as a function of frequency measured in periods per day. Selected stations are representative of the three wind-climate types in Slovenia: almost 1500 m elevated RO, PO station at the Adriatic coast and a valley station SG. A largest amount of the wind power is measured at the exposed mountaintop (RO) – almost twice that at PO and about seven times that at SG stations (Fig. 6).

There is a major difference between the spectral power distribution in the three temporal ranges at various places. The diurnal circulation on the mountain station is non-significant (makes only 2%), it is relatively weak also in the valley (SG) (7%), but it dominates the observed spectrum at the coast (sea breeze); there

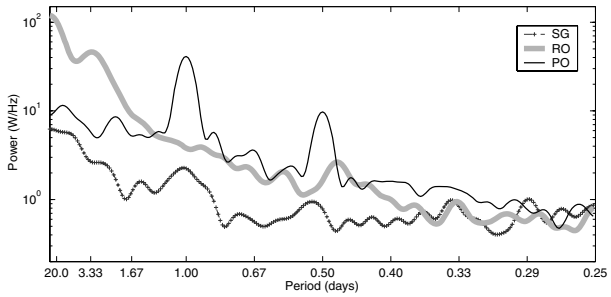

Fig. 6. Spectral power distribution as a function of frequency for the observed zonal wind at the three stations. Dashed line with + symbols belongs to the spectrum at the valley station SG, the mountaintop station RO is shown in grey, whereas thin black line corresponds to the spectrum at the coastal station PO.

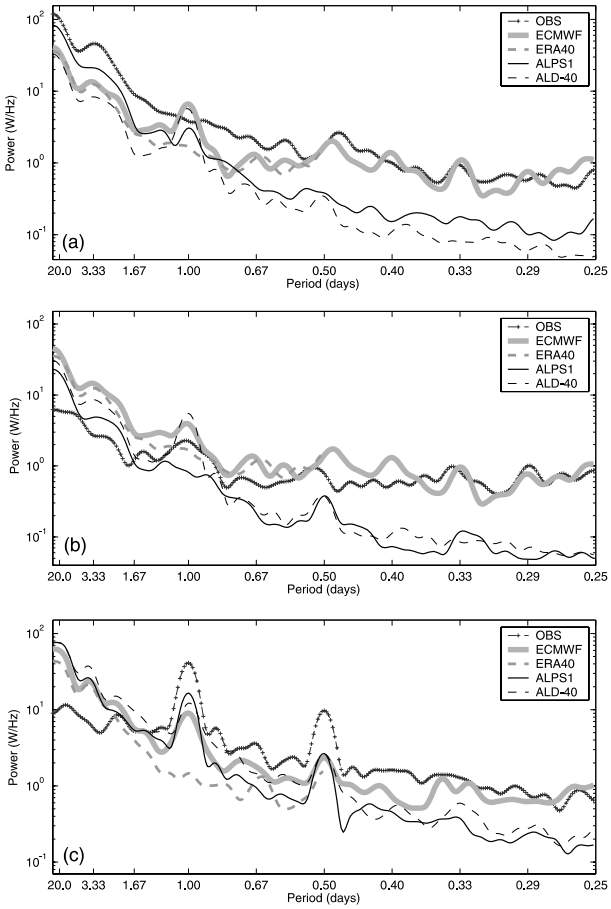

Fig. 7. Observed versus modelled power spectra for the zonal wind component at stations (a) RO, (b) SG, and (c) PO. The observed spectrum is presented by dashed line with + symbols, the ECMWF models are shown in grey (thick full line for MAP reanalysis and dashed line for ERA40), whereas thin black line corresponds to the ALADIN spectra (full line to directly nested ALPS simulation and dashed line to 40 km ALADIN).

it contributes 28% of the power. The subdiurnal range contributes the largest part of the spectrum in the valley (41%), while LTD periods are dominant at the mountain site (86%).

A successful downscaling model should have its spectral power distribution as close as possible to the observed distribution, and the amount of power in each time range as similar as possible to the measured amount. These expectations can be checked in Fig. 7 for the three stations and the two horizontal resolutions. Among various ALADIN simulations the results of the ALPS1 experiment are chosen to be presented, but the spectra look very similar for other two experiments (ALPS2 and EU1).

At RO, well exposed to the large-scale flow, the models underestimate the power in all frequencies except for ECMWF reanalysis in periods below 12 hr. It can be seen in Fig. 7a how an increased horizontal resolution (ECMWF and ALD-40 vs. ALPS), that is, raising up the station height above the sea level (550 m vs. 1120 m), acts to produce a more realistic power profile in the LTD band. Both observations and the models display a maximum of the spectral power at a period of about 3 d, typical for synoptic perturbations. There is a local minimum at 5.4 d period after which the power steadily grows towards longer periods.

The largest discrepancy between ALADIN and ECMWF is found in the subdiurnal range. Although there is relatively little power in this part of the spectrum, it is an interesting and unexpected feature. The lack of variability in the subdiurnal range of ALADIN is further confirmed in Fig. 7b showing spectra at SG, a station with about 40% of the observed power in this band. This feature is not something unambiguous for this 70 d data set since yearly time-series for both observations and ALADIN display the same characteristics. As possible causes for this behaviour we excluded an insufficient spin-up time (by performing a 999-hr-long continuous simulation on the EU1 domain) and the strength of lateral boundary forcing (spectra from larger domains look very similar). Another possibility is that ALADIN has numerical filtering so strong that it removes the input from physical processes on smaller scales. Favouring this hypothesis is a spectrum of the kinetic energy, which remains close to a k^{-3} behaviour all the way down to the lowest resolvable scale ($3\Delta x$ in the spectral ALADIN).

The LTD periods are overestimated at SG since this north–south-oriented valley is not properly resolved at the horizontal resolution of 10 km. When we apply the dynamical downscaling of Žagar and Rakovec (1999) to produce the wind field at 2.5 km, the power in LTD band significantly reduces and becomes even smaller than that in the observations. The subdiurnal range, however, remains poorly represented since this method is a pure dynamical adjustment to a new terrain (not shown).

Downscaling of ERA40 influences the diurnal peak in the power profile by making it stronger at all stations; this can be seen in the RO spectra and especially at the coastal station PO (Fig. 7c). Here, the power in LTD band, available in driving ERA40 fields, has not been reduced in ALADIN. However, the

diurnal and subdiurnal power bands due to the sea-breeze circulation are simulated realistically. Instead of see breeze, the power spectrum of the ERA40 time-series presents a local maximum at the frequency of the inertial oscillation (about 16 hr). It is also interesting to notice the presence of a significant diurnal component in the spectra of MAP-SOP reanalyses (denoted ECMWF) and ALD-40.

A more quantitative comparison of the observed and modelled spectral power in the zonal wind component is provided in Fig. 8, which shows spectral power distribution in different ranges, normalized by the total power (x-axis) and by the observed power in the same frequency range (y-axis) (at the same station). This figure thus summarizes information about the spectral power distribution as a function of the model definition and the realism of this result.

If we first pay attention to the x-axis dependence and observations (denoted by filled circles), it can be noted that stations are grouped into a group of three (mountaintop) stations (three points most to the right in Fig. 8a and most to the left in Fig. 8c), one isolated point (coastal station, a point most to the right in 8b) and the rest (valleys and basins). The distribution of spectral power among three temporal regimes is similar to the one reported in RDL2004. Stations in valleys and lowlands contain 30–40% of their power in the subdiurnal range and 40–60% in LTD periods. At three mountain stations LTD periods or synoptic and longer timescale perturbations contribute over 80% of the spectral power. The diurnal range is not significant except at PO, where the sea breeze dominates circulation.

On the other hand, the modelling results do not display such a distinct difference between various wind climate areas. The wind power modelled by ALADIN is mainly in LTD periods as provided by ERA40 forcing fields. The model thus significantly overestimate LTD part of the spectra except at three mountain stations. Spectra verification do not discriminate between ALADIN at 10 km and ALD-40, in contrast to the conventional scores shown in Fig. 5. Thus, Fig. 8c illustrates that increasing horizontal resolution from 40 to 10 km is not necessarily enhancing the temporal variability of circulations, contrary to what we expected as a result of the terrain and thermal forcings.

At the same time, the MAP-SOP reanalyses dispose relatively more power than ALADIN in the subdiurnal range (Fig. 8c). For example, the station with the largest percentage of subdiurnal power in ALPS1 simulation is BR; here, 19% of the modelled power is in the subdiurnal band, but this makes only 29% of the observed subdiurnal power at this location. In the same frequency range BR observations contain 43% of power. The ratio between the modelled and measured LTD power content at BR is very close to one, but respective values amount to 75% of the modelled and 47% of the observed power. Except at a single coastal station, circulations with diurnal periods make up a small part of the spectra. This applies to the observations and, to an even larger extent, to the models (Fig. 8b).

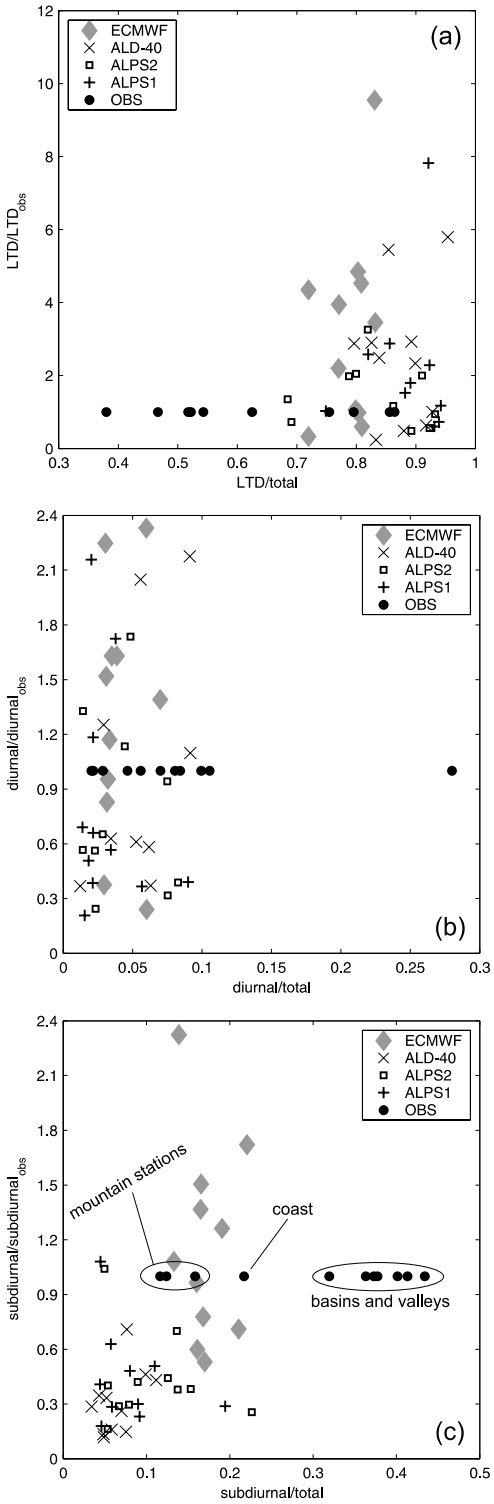

Fig. 8. Spectral wind power at each station in the (a) longer than diurnal, (b) diurnal and (c) subdiurnal periods normalized by the spectral power in the same frequency range in observations, plotted against the power in a particular spectral range normalized by the total power at the station. Figure legend associates symbols with various simulations, the names are explained in Table 1 and in the text.

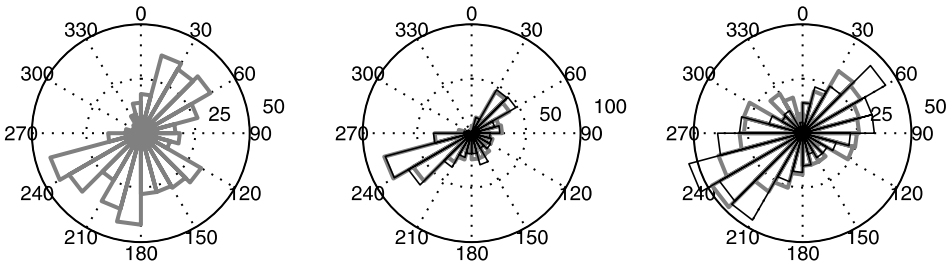

Fig. 9. Wind roses from (left) observations, (middle) ALADIN-ALPS1, and (right) MAP reanalyses at the well-exposed station LI during the 70 d MAP-SOP period (thick lines). Thin lines: wind roses after the time-series were smoothed by a 12 hr running average. Numbers belonging to the rings indicate percentages.

The importance of the subdiurnal range at the majority of our stations and the absence of the power in this low-predictability range in the model may also explain a similarity between the results for the directly nested domain (ALPS1) and one nested into an intermediate domain (ALPS2).

3.3. Subdiurnal variability

In this subsection we further investigate the difference in the subdiurnal range between the ECMWF and ALADIN models. Figure 9 suggests that a significant amount of the spectral power in the subdiurnal range in MAP reanalyses is associated with an increased variability of the wind direction in the ECMWF model compared to ALADIN, in spite of a four times lower resolution. Wind roses in Fig. 9 are representative for the mountain station LI, but narrower wind roses in ALADIN simulations than in ECMWF are found at almost all stations.

To find out the exact reasons for differences in the subdiurnal range is out of the scope of the present paper. We can, however, ask how are a better reconstruction of the observed wind roses and an increased power content in the subdiurnal range (with respect to ALADIN) related to the conventional scores of MAP reanalyses? The answer is provided in Fig. 10 comparing the MAEs from ECMWF and ALPS simulations with those obtained after times-series were smoothed by a 12 hr running average. It can be seen that the error of ECMWF has been significantly reduced, in average for about 20% of its initial value. New scores are closer to ALADIN, especially RMSE scores (not shown). Filtering ALD-40, on the other hand, changed the scores to a much smaller extent, while those for ALPS simulations were almost unaffected by filtering and are thus not shown in figure. Wind roses for filtered data are more narrow, but still more variable in ECMWF than in ALADIN (Fig. 9).

Examining the model time-series at various stations, it is seen that the improvement shown in Fig. 10 is mainly due to short-period oscillations present in the original time-series from MAP-SOP reanalyses. The oscillations are not a consequence of the post-processing to 10 m height, since the

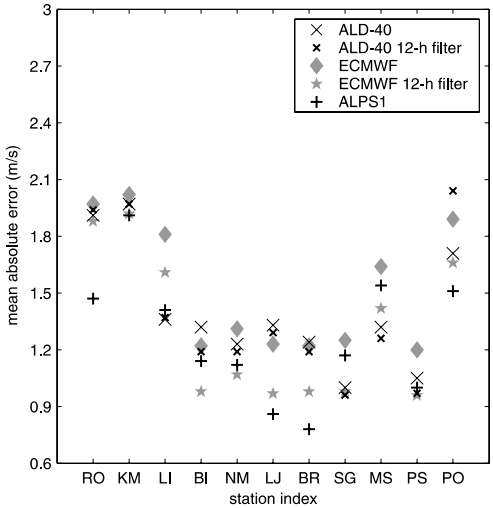

Fig. 10. As Fig. 5a, but including filtered time-series from MAP reanalyses and ALD-40.

same behaviour characterizes the lowest model levels (levels 58–60). The power spectrum of the filtered time-series is found below the curve for ALADIN in the subdiurnal range (Fig. 11). For further comparison, we applied the spectral analysis also on the forecasts initiated from MAP reanalyses (for same forecast range 12–60 hr). Although the sampling was only 6 hr because of data availability, the available subdiurnal part of the spectra (periods above 12 hr) contain less energy than corresponding curves for ALADIN. In conclusion, subdiurnal variability, present in near surface wind field in the MAP-SOP reanalysis data, is damaging for its scores; it is noise introduced in the assimilation cycle possibly by supplementary data. Such conclusion is further supported by the scores of ALD-40 in Fig. 5, which at most stations are better than those from MAP reanalyses.

It has to be noted that a validation of LAM forecasts with global model analyses is in general a questionable approach. We are verifying post-spin-up adaptation of ALADIN, that is, periods where the influence of the observed data enters only via LBC

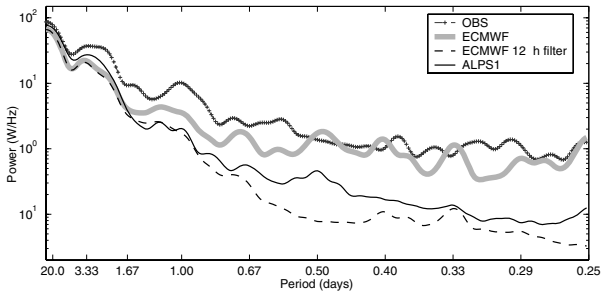

Fig. 11. As Fig. 7, but for the station LI and including the filtered MAP reanalysis time-series (black dashed line).

and not any more via initial plus LB conditions, versus a continuous data assimilation cycle. Even in a small domain such as ALPS, there is still an upstream and a downstream component to the LBC influence, especially for complex signals propagating at different speeds. In other words, our observation at time $t = 0$ will not necessarily significantly influence the state of the LBC upstream; thus the LBC used at +24 hr for coupling an ALADIN simulation do not 'feel' this refreshment while the MAP-SOP reanalysis does. In favour of this explanation we notice that the gap between the ALADIN and ECMWF in the subdiurnal frequency band is somewhat smaller for the meridional than for the zonal wind component, which is in this geographical region more influenced by LBC, as well as that the wind variability in ALADIN is somewhat larger in a larger domain (EU1 versus ALPS). In this paper, however, we believe that using MAP reanalyses was appropriate as it allowed us to better quantify the impact of downscaling of ERA40. Furthermore, we were able to show that an increased variability in the subdiurnal range of MAP reanalysis, in comparison with ALADIN, is detrimental for its scores. Power inserted in the subdiurnal band during assimilation seems to be removed by the model numerics during the early stage of the forecasts.

4. Summary and Conclusions

For the present paper we defined two goals. First, a frequency-domain verification has been applied to explore aspects of the mesoscale model performance other than that depicted by the conventional statistics. Secondly, we aimed at defining the optimal strategy for nesting the ALADIN model into ERA40 which produces the most realistic wind field in the complex terrain of Slovenia.

Modelled wind fields are compared with the time-series of observations at 11 Slovenian stations. The verification period is the Special Observing Period of the Mesoscale Alpine Program (MAP-SOP), for which reanalyses including MAP-SOP observations were produced by the continuous data-assimilation system of ECMWF and are available every 3 hr on a ∼40 km grid. The comparison of wind time-series resulting from MAP reanalyses and ALADIN provides additional information concerning the importance of horizontal resolution as compared to other modelling aspects.

A frequency-domain comparison allows quantifying the observed circulation in terms of subdiurnal, diurnal and LTD periods. In this way, three distinctive wind climate areas became evident including the exposed mountaintop stations, characterized by over 80% of their spectral power in LTD periods, the Adriatic coast, dominated by the sea-breeze circulation, and the rest of Slovenia, with its valleys, basins and lowlands, containing about 40% of power in the subdiurnal and about 50% in LTD periods.

There are three relevant conclusions summarized as follows. First of all, the comparison of ALADIN outputs with observations and MAP reanalyses shows a clear improvement of the conventional statistics based on the mesoscale model as compared to 40 km analyses and persistence forecast. The intercomparison of various ALADIN simulations shows that a smaller horizontal domain produces better scores and that scores are not better for a two-step nesting than for a direct one, in spite of a ratio of horizontal resolutions in ERA40 and ALADIN as large as 12.

A more physical insight is attempted through a comparison of the observed and modelled spectra in the frequency domain. It is suggested that a part of the error is due to the fact that a majority of the stations is characterized by about 40% of their spectral wind power in the subdiurnal frequency range, which is poorly represented by ALADIN and is generally characterized by a low predictability. This conclusion is strengthened by the scores at mountaintop stations showing little sensitivity to the domain size and nesting strategy. The model places less than 10% of its spectral power in the subdiurnal range; that is, too much power is retained in the LTD part of the spectrum, which is suitable only for the mountaintop stations. This means that the dynamical downscaling in our case is predominantly an adjustment to the new terrain, while physical process due to increased resolution are of secondary importance.

On the other hand, and in spite of a four times lower resolution, the ECMWF model places twice more power than ALADIN in the subdiurnal frequency range and produces wind roses closer to observations. However, this power has been shown to be due to unrealistic oscillations present in the MAP reanalysis, and after their filtering the conventional scores for MAP reanalyses improved significantly.

Finally, based on the presented results we suggest that the applied verification methodology may have some relevance for regional climate simulations and estimates of the representativity of observing stations used in verification studies. Given the time-series of observations and a mesoscale model, a perpetual simulation that is, a spectral decomposition of simulated time-series may provide useful information about a model's general ability to simulate observations. This methodology may also serve as a tool used for estimating a minimal domain size sufficient for the development of mesoscale features that can be simulated by a model at hands.

In the particular case presented, an area of complex orography and strong surface gradients, it is concluded that only three well-exposed mountain stations are insensitive to the regional model domain definition and their wind power spectra is well represented by the applied mesoscale model. A majority of stations is located in valleys and basins and it is characterized by a significant variability on the subdiurnal scales; these processes can hardly be resolved by most of present-day NWP models. Therefore, these stations have a limited use in the regional wind climate modelling and studies of future wind climates.

5. Acknowledgments

The authors would like to thank Jean-Françcois Geleyn, Branko Grisogono and Daran Rife for reading the earlier version of this paper and for their relevant comments, and to them and Dieter Heimann, Filip Váña and Pedro Viterbo for discussions related to various aspects of this study. Reviewers' comments and constructive criticism which led to the paper improvements are highly appreciated.

References

Beck, A., Ahrens, B. and Stadlbacher, K. 2004. Impact of nesting strategies in dynamical downscaling of reanalysis data. *Geophys. Res. Let.* **31**, L19101, doi:10.1029/2004GL020115.

Bougeault, P., Binder, P., Buzzi, A., Dirks, R., Houze, R. and co-authors. 2001. The MAP Special Observing Period. *Bull. Am. Meteorol. Soc.* **82**, 433–462.

Brzović, N. 1999. Factors affecting the Adriatic cyclone and associated windstorms. *Contr. Atmos. Phys.* **72**, 51–65.

Bubnova, R., Hello, G., Benard, P. and Geleyn, J.-F. 1995. Integration of the fully elastic equations cast in the hydrostatic pressure terrain-following coordinate in the framework of the ARPEGE/ALADIN NWP system. *Mon. Wea. Rev.* **123**, 515–535.

Denis, B., Larprise, R. and Caya, D. 2003. Sensitivity of a regional climate model to the resolution of the lateral boundary conditions. *Clim. Dyn.* **20**, 107–126.

Ghil, M., Allen, M. R., Dettinger, M. D., Ide, K., Kondrashov, D., and co-authors. 2002. Advanced spectral methods for climatic time series. *Reviews of Geophysics* **40**, doi:10.1029/2001RG000092.

Heimann, D. 2001. A model-based wind climatology of the eastern Adriatic coast. *Meteorol. Z.* **10**, 5–16.

Jones, R. G., Murphy, J. M. and Noguer, M. 1995. Simulation of climate change over Europe using a nested regional-climate model: I: assessment of control climate, including sensitivity to location of lateral boundaries. *Q. J. R. Meteorol. Soc.* **121**, 1413–1449.

Kållberg, P., Simmons, A., Uppala, S. and Fuentes, M. 2004. The ERA-40 archive. *ECMWF ERA-40 Project Report Series* **17**, 1–35.

Keil, C. and Cardinali, C. 2004. The ECMWF reanalysis of the MAP Special Observing Period. *Q. J. R. Meteorol. Soc.* **130**, 2827–2849.

Mass, C. F., Ovens, D., Westrick, K. and Colle, B. A. 2002. Does increasing horizontal resolution produce more skillful forecast? *Bull. Am. Meteorol. Soc.* **83**, 407–430.

Qian, J.-H., Seth, A. and Zebiak, S. 2003. Reinitialized versus continuous simulations for regional climate downscaling. *Mon. Wea. Rev.* **131**, 2857–2874.

Rife, D. L., Davis, C. A. and Liu, Y. 2004. Predictability of low-level winds by mesoscale meteorological models. *Mon. Wea. Rev.* **132**, 2553–2569.

Steinacker, R., Häberli, C. and Pöttschacher, W. 2000. A transparent method for the analysis and quality evaluation of irregularly distributed and noisy observational data. *Mon. Wea. Rev.* **128**, 2303–2316.

Žagar, M. and Rakovec, J. 1999. Small-scale surface wind prediction using dynamic adaptation. *Tellus* **51**, 489–504.